JOURNAL OF COLLOID AND INTERFACE SCIENCE 168, 402–413 (1994)

Nonlinear Solutal Marangoni Instability in a Liquid Layer with an Adsorbing Upper Surface

J. BRAGARD,* S. G. SLAVTCHEV,† AND G. LEBON*,[1]

*Institute of Physics, Liege University, Sart Tilman B5, B-4000 Liege, Belgium; and
†Institute of Mechanics, Bulgarian Academy of Sciences, 1113 Sofia, Bulgaria

Received January 28, 1994; accepted May 12, 1994

Nonlinear solutal convection in a thin liquid layer driven by surface-tension gradients is studied. This effect is referred to as the Marangoni effect. The adsorbing ability of the upper surface is described by the Gibbs adsorption equation. The present analysis is based on the amplitude method, which allows for finite amplitude disturbances. The nonlinear terms are stabilizing or destabilizing according to the adsorption characteristics of the upper boundary. The present study generalizes earlier linear analyses. The nature of the convective pattern is also determined: it is shown that a hexagonal rather than a roll symmetry is expected.

1. INTRODUCTION

Spontaneous convection driven by surface-tension gradients due to mass transfer through a gas–liquid or a liquid–liquid interface (Marangoni effect) is recognized as an important factor for enhancing mass transfer rates (1–3). The influence of Marangoni convection in mass transfer problems was observed by Sawistowski (2) and Linde *et al.* (3). Sternling and Scriven (4) were the first to propose a theoretical treatment about the role of interfacial phenomena on mass transfer processes. They found that induced organized cellular motion in both phases near the interface is due to a nonhomogeneous distribution of solute at the interface and predicted the occurrence of roll cells which are analogous to those observed in a horizontal layer of pure fluid heated from below (5). The experimental verification of Sternling and Scriven's results was provided by Linde (3, 6), but his checking was valid only for thin liquid layers at the very beginning of the fluid motion. After a short time (of the order of 20 to 30 s.) drifting cells of different shapes are emerging. In thick layers, Orell and Westwater (7) observed polygonal cells with three to seven or more sides which, in contrast to Linde's observations, might persist during very long times, up to 15 h.

Sternling and Scriven's work (4) was generalized to deformable and spherical interfaces (8–13) as well as to systems involving surface (14–18) or volume (19) chemical reactions. Pearson's linear stability analysis (20), valid for thermocapillary convection, was extended by Brian *et al.* (21–23), who studied gas desorption from a liquid. Brian and his collaborators based their approach on the Gibbs adsorption mechanism. However, their results are not in agreement with the experimental results of Imaishi *et al.* (24, 25) concerning desorption of some organic liquids. Imaishi *et al.* found a finite critical Marangoni number for values of the adsorption number N_A (for a precise definition of N_A see Section 2) at which the Marangoni number should be infinite, according to Brian's linear theory. The discrepancy may be explained by the crudeness of the linear models. Experiments on cellular convection at the interface between fluids have also been conducted by Palmer and Berg (26).

To our knowledge, a nonlinear stability analysis of mass transfer through interfaces has not been developed yet. Concerning the nonlinear thermal Marangoni problem, several approaches have been proposed (5, 27–30). The first was developed by Scanlon and Segel (27), who used a successive approximation technique. Scanlon and Segel assumed that the liquid layer is of semi-infinite depth and considered an infinite Prandtl number. The restriction about an infinite depth was relaxed in a recent paper by Bragard and Lebon (31), who confirmed the general trends of Scanlon and Segel's work but obtained slightly different values for the relevant stability parameters.

In the present work, Bragard and Lebon's nonlinear formalism (31) is applied to study the solutal Marangoni convection resulting from mass transfer through the gas–liquid upper surface of a thin liquid layer. The motivations behind the present work are twofold: first, to examine to which extent results obtained for thermal instability are transposable to solutal convection, and second, to check whether the emergence of convective planforms as observed experimentally is confirmed by a theoretical approach. In the case of mass transfer, the simplifying restriction of an infinite Prandtl number is replaced by the equivalent assumption of a very large Schmidt number, which is known to be fulfilled by many chemical systems.

[1] To whom correspondence should be addressed.

0021-9797/94 $6.00

The system under consideration consists of a thin liquid layer whose upper surface, in contact with an inert gas phase, is flat but subject to a chemically surface-active components transfer. The absorbing ability of the gas–liquid surface is described by the Gibbs adsorption equation (21–23, 32). A bulk diffusion-controlled transfer in the liquid phase and an adsorption–desorption-controlled gas–liquid transfer at the upper boundary are assumed.

The present analysis is restricted to weakly nonlinear interactions: only the second-order approximation is investigated. The problem treated here differs from Marangoni's thermal convection because the motor of instability is now a mass gradient rather than a temperature gradient. As a consequence the energy balance equation is replaced by a mass balance equation and supplementary boundary conditions expressing the exchange of matter at the free surface are introduced. Moreover, in addition to Marangoni solutal number another relevant nondimensional parameter will be incorporated, namely the adsorption number representing the surface convection of the solute (21).

2. STATEMENT OF THE PROBLEM

Consider a liquid layer of thickness d and infinite horizontal extent; the layer is bounded below by a rigid plate and above by a free surface in contact with a gas phase. Mass transfer of a given chemical component takes place through the upper boundary. Gravity effects are neglected, which is certainly a good approximation for very thin layers. Both adsorption of a gas component into the layer and desorption of a solute into the gas phase are considered. The bulk velocity of the gas phase is assumed to be negligible and the mass transfer from (to) it to (from) the gas–liquid surface is modeled by a constant mass transfer coefficient, called the gas–liquid Biot number. It is supposed that the solution is surface-active and that its surface tension σ depends linearly on the concentration excess according to the law (21)

$$\sigma = \sigma_r - \alpha(c - c_r), \qquad [1]$$

where c_r is an arbitrary reference concentration and α a constant; approximation [1] is justified at rather low concentrations.

Since our analysis is restricted to dilute solutions, it is a good assumption to suppose that the liquid viscosity μ and density ρ are constants, from which follows that the liquid is Newtonian and incompressible. The thermal effect related to the adsorption (desorption) process is neglected and as a consequence Marangoni thermal instability is excluded. The free surface is taken to be planar and undeformable.

In the basic unperturbed state the fluid is at rest, the surface concentration is constant, and the bulk concentration c_0 is linearly distributed across the layer. Using Cartesian coordinates x, y, z with axes $\mathbf{x}$ and $\mathbf{y}$ in the bottom wall and axis $\mathbf{z}$ directed toward the free surface, one has (21)

$$c_0 = c_w - \beta z,$$

where c_w is the concentration at the bottom wall and β the constant concentration gradient; β is positive in the case of desorption and negative when the gas surfactant is adsorbing.

According to Gibbs adsorption mechanism (21, 32), there exists within the range of small concentrations a linear adsorption approximation

$$\Gamma = \left(\frac{\alpha}{RT}\right) c_i \equiv \delta c_i, \qquad [2]$$

between the surface concentration Γ and the bulk concentration c_i in the vicinity of the surface, Γ represents the number of moles of solute per unit surface adsorbed at the interface, α is the negative of the slope of the curve giving the surface tension versus the solute concentration, R is the ideal gas constant, T is the equilibrium temperature, and δ is a constant whose dimension is that of a length. The surface adsorption Γ satisfies a boundary condition expressing the balance of mass of the solute at the free interface and given by (19, 29)

$$-D_L \frac{\partial c}{\partial z} - Hk_g(c - c_g) = \frac{\partial \Gamma}{\partial t} - D_s \nabla_1^2 \Gamma + \frac{\partial}{\partial x}(u\Gamma) + \frac{\partial}{\partial y}(v\Gamma) \quad (z = d). \qquad [3]$$

The following notation is used: t is the time, u and v are the fluid velocity components with respect to the axes $\mathbf{x}$ and $\mathbf{y}$, c_g is the surfactant concentration in the gas phase far from the surface, D_L and D_s are the bulk and surface diffusion coefficients in the liquid phase and the surface layer, respectively, H is Henry's law constant, k_g is the gas-phase mass transfer coefficient, and $\nabla_1^2 = \partial_{xx}^2 + \partial_{yy}^2$ is the two-dimensional Laplacian. For desorption, for example, the first term on the left-hand side of [3] represents the net rate of solute transferred from the bulk to the surface; the second term in the left-hand side represents the transfer from the interface to the gas phase containing the solute component at a partial pressure corresponding to the liquid phase concentration c_g. These two terms are equivalent to Newton's cooling law for heat transfer. The terms on the right-hand side of [3] represent the effect of Gibbs adsorption: the first term on the right-hand side of [3] represents the solute accumulation at the interface, the second term describes surface diffusion, and the last two terms are related to surface convection of the solute in the adsorbed layer.

To formulate the stability problem it is convenient to express the variables in dimensionless form. With scaling distance, time, velocity $\mathbf{v}$ (u, v, w), and bulk concentration given by d, d^2/D_L, D_L/d, and βd, respectively, the governing

dimensionless equations for the velocity and concentration disturbances are given by (24)

$$\nabla^4 w = \mathrm{Sc}^{-1}[\nabla^2 w + \nabla_1^2(\mathbf{v}\cdot\nabla w) - \partial_{xz}(\mathbf{v}\cdot\nabla u) - \partial_{yz}(\mathbf{v}\cdot\nabla v)], \quad [4]$$

$$\nabla^2(\nabla_1^2 u + \partial_{xz} w) = \mathrm{Sc}^{-1}[\partial_t(\nabla_1^2 u + \partial_{xz} w) + \partial_{yy}(\mathbf{v}\cdot\nabla u) - \partial_{xy}(\mathbf{v}\cdot\nabla v)], \quad [5]$$

$$\nabla^2(\nabla_1^2 v + \partial_{yz} w) = \mathrm{Sc}^{-1}[\partial_t(\nabla_1^2 v + \partial_{yz} w) + \partial_{xx}(\mathbf{v}\cdot\nabla v) - \partial_{xy}(\mathbf{v}\cdot\nabla u)], \quad [6]$$

$$\partial_t c + (\mathbf{v}\cdot\nabla c) = w + \nabla^2 c, \quad [7]$$

where $\nabla^2 = \nabla_1^2 + \partial_{zz}^2$, and $\mathrm{Sc} = \mu/\rho D_L$ is the Schmidt number; for convenience we have kept the same notation for the dimensional and dimensionless quantities. Equations [4]–[6] represent the components of the momentum balance after use is made of the continuity equation. Equation [7] is the mass balance law wherein c designates the difference between the actual concentration and its unperturbed value c_0.

Within the hypothesis of large values of the Schmidt number Sc (a reasonable assumption), one can neglect the terms on the right-hand side of [4]–[6]. The quantities between brackets on the left-hand side of [5] and [6] are harmonic functions with zero normal derivatives at the free surface and zero values at the bottom surface; this means that they vanish everywhere in the layer and it follows that

$$\nabla_1^2 u = -\partial_{xz} w, \quad \nabla_1^2 v = -\partial_{yz} w. \quad [8]$$

Moreover for infinitely large values of Sc, relation [4] reduces to

$$\nabla^4 w = 0, \quad [9]$$

so that nonlinear terms are present only in the diffusion equation [7].

Equations [7]–[9] satisfy the following boundary conditions. At the rigid lower wall ($z = 0$), the no-slip condition imposes that

$$u = v = w = 0, \quad [10]$$

while the bulk concentration satisfies either

$$c = 0 \text{ ("conducting" case)}, \quad [11]$$

or

$$\partial_z c = 0 \text{ ("insulating" case)}. \quad [12]$$

Condition [11] is achieved if the bottom is visualized as a semipermeable membrane through which the solute diffuses infinitely rapidly from a supply solution located beneath the membrane (21). Expression [12] means that there is no flux of matter through the wall.

At the upper interface, the kinematics condition expressing nondeformability is given by

$$w = 0, \quad [13]$$

and at high Schmidt numbers, the balance of the tangential forces takes the form (33, 34)

$$\frac{\partial^2 w}{\partial z^2} - \mathrm{Ma}\nabla_1^2 c = 0, \quad [14]$$

where

$$\mathrm{Ma} = \alpha\beta d^2/\mu D_L \quad [15]$$

is the solutal Marangoni number. Expression [14] implies that surface shear and dilatational viscosity are small, which is justified for very low values of Γ. Boundary conditions [10]–[14] are complemented by boundary condition [3], which in linear form is written as (21)

$$\partial_z c + \mathrm{Bi}\, c - N_A \partial_z w = -\tilde{\delta}\partial_t c + S\nabla_1^2 c, \quad [16]$$

after that Gibbs' law [2] has been used; the dimensionless gas–liquid Biot number Bi and the so-called *adsorption number* N_A are defined by

$$\mathrm{Bi} = \frac{k_g H d}{D_L}, \quad N_A = \frac{\Gamma_0}{\beta d^2}, \quad [17]$$

where the undefined quantities $\tilde{\delta}$ and S are given by $\tilde{\delta} = \delta/d$ and $S = \delta D_s/dD_L$, and Γ_0 ($=\delta c_0$) is the surface concentration in the unperturbed state. The dimensionless groups $\tilde{\delta}$ and S stand for the relative depth of the Gibbs layer and the surface diffusion, respectively. As $\tilde{\delta}$ and S are very small quantities without influence on the stability problem (18), they will be taken equal to zero. By writing [16], we have neglected the nonlinear terms $u\Gamma$ and $v\Gamma$ as involving only the products of two infinitesimally small disturbances.

We are thus left with a set of four partial differential equations [7]–[9] together with boundary conditions [10], [14], and [16]. The problem investigated here generalizes that of nonlinear thermal Marangoni instability (27, 31), the essential differences lying in the boundary condition [16] and the physical interpretation of the various parameters. In the conducting case one should recover the results of Ref. (31) by setting $N_A = 0$.

3. SOLUTION OF THE PROBLEM

The problem is solved by means of an iterative process. Let us introduce the notation (27, 31)

$$\mathbf{L} = \begin{bmatrix} \nabla^4 & 0 & 0 \\ 1 & \nabla^2 & 0 \\ \partial^2_{zz}|_{z=1} & 0 & 0 \end{bmatrix},$$

$$\mathbf{N} = \begin{bmatrix} 0 & 0 & 0 \\ 0 & \partial_t + \mathbf{v}\cdot\nabla & 0 \\ 0 & 0 & 0 \end{bmatrix}, \quad \mathbf{M} = \begin{bmatrix} 0 & 0 & 0 \\ 0 & 0 & 0 \\ 0 & 0 & \nabla_1^2 \end{bmatrix}. \quad [18]$$

In terms of these operators, Eqs. [7], [9], and [14] are written as

$$\mathbf{L}(\mathbf{u}) = \mathbf{N}(\mathbf{u}) + \mathrm{Ma}\mathbf{M}(\mathbf{u}), \quad [19]$$

where $\mathbf{u}$ is the perturbation vector with components

$$\mathbf{u} = [w(x, y, z, t), c(x, y, z, t), c(x, y, 1, t)]. \quad [20]$$

For future purpose, it is also necessary to define the scalar product of two vectors $\mathbf{a} = (a_1, a_2, a_3)$ and $\mathbf{b} = (b_1, b_2, b_3)$ by

$$\langle \mathbf{a}, \mathbf{b} \rangle = \lim_{l\to\infty} \frac{1}{4l^2} \int_{-l}^{l}\int_{-l}^{l} dx\, dy \times \left[a_3 b_3 + \int_0^1 dz (a_1 b_1 + a_2 b_2) \right], \quad [21]$$

wherein l represents the horizontal extent. To ensure the convergence of the iterative scheme, expression [19] is rewritten in the form

$$[\mathbf{L} - \mathrm{Ma}^c\mathbf{M}](\mathbf{u}^{(n)}) = [\mathbf{N} + (\mathrm{Ma} - \mathrm{Ma}^c)\mathbf{M}](\mathbf{u}^{(n-1)}), \quad [22]$$

where the right-hand side contains only small terms and where Ma^c is the critical value of the Marangoni number obtained from the linear theory. Defining the distance to the stability threshold by $\epsilon = (\mathrm{Ma} - \mathrm{Ma}^c)/\mathrm{Ma}^c$, it is expected that convergence will be ensured for sufficiently small values of ϵ.

3.1. *Linear Solution*

The first step consists of solving the linear problem corresponding to $n = 1$ and $\mathbf{u}^{(0)} = 0$. The solution can be cast in the form

$$\mathbf{u}^{(1)} = [W_1(z), C_1(z), C_1(1)]\Phi(x, y, t), \quad [23]$$

wherein the planform function Φ is a solution of the Helmholtz equation

$$\nabla_1^2\Phi + a^2\Phi = 0, \quad [24]$$

with a the dimensionless wave number. Setting $D = d/dz$, the functions $W_1(z)$ and $C_1(z)$ satisfy the equations and boundary conditions

$$(D^2 - a^2)^2 W_1 = 0 \quad [25]$$

$$(D^2 - a^2)C_1 = -W_1 \quad [26]$$

$$W_1 = DW_1 = 0,\ DC_1 + \mathrm{Bi}C_1 = 0 \quad \text{at } z = 0, \quad [27]$$

$$W_1 = 0,\ DC_1 - NaDW_1 + \mathrm{Bi}C_1 = 0,$$
$$D^2W_1 + a^2\mathrm{Ma}C_1 = 0 \quad \text{at } z = 1. \quad [28]$$

The expressions for $W_1(z)$ and $C_1(z)$ are derived by Pearson (20),

$$W_1(z) = A\{[1 + (a\coth a - 1)z] \times \sinh az - az\cosh az\} \quad [29]$$

$$C_1(z) = b_1\sinh az + b_2\cosh az - A\left[\frac{3z}{4a}\cosh az - \frac{z^2}{4}\sinh az + \frac{a\coth a - 1}{4a^2}(az^2\cosh az - z\sinh az)\right], \quad [30]$$

where A, b_1, and b_2 are arbitrary constants. Making use of boundary conditions [27c] and [28b], it is possible to express the constants b_1 and b_2 in terms of A. Condition [28c] gives the solubility condition for the eigenvalue problem and results in the expression of the Marangoni number in terms of the wave number, the Biot number, and the adsorption numbers. In the conducting case ($c = 0$ at the bottom), it is found that the neutral curve Ma versus a is given by

$$\mathrm{Ma} = \frac{8a(\sinh a\cosh a - a)(a\cosh a + \mathrm{Bi}\sinh a)}{(\sinh^3 a - a^3\cosh a) - 4N_A a^2\sinh a(\sinh^2 a - a^2)}. \quad [31]$$

In the insulating case ($\partial_z c = 0$ at the bottom), one obtains

$$\mathrm{Ma} = \frac{8a(\sinh a\cosh a - a)(a\sinh a + \mathrm{Bi}\cosh a)}{\cosh a(a^2 + \sinh^2 a) - a(2 + a^2)\sinh a - 4N_A a^2\cosh a(\sinh^2 a - a^2)}. \quad [32]$$

Combining Gibb's law [2] and the definition [17b] of N_A results in

$$N_A = \frac{\alpha c_0}{\beta RTd^2}. \quad [33]$$

The dimensionless numbers Ma and N_A have the same sign because the quantities α and β (which may be positive or

negative separately) enter the former as a product and the latter as a ratio. For negative values of N_A, neutral stability curves are found for positive Ma values (21), which corresponds to unphysical situations: this means that systems with $N_A < 0$ and $Ma < 0$ are always stable. So, adsorption of surface-tension-decreasing solute (corresponding to $\beta < 0$ and $\alpha > 0$) and desorption of surface-tension-increasing solute ($\beta > 0$ and $\alpha < 0$) are stable as confirmed experimentally (24).

Consider now positive values of N_A. The minimum value of the neutral stability curve yields the values of the critical Marangoni number Ma^c and the critical wave number a^c: in the conducting case the critical Marangoni number Ma^c is positive for $0 \leqslant N_A < 0.05$ and tends to infinity when N_A approaches 0.05 (19); in the insulating case the corresponding interval is $0 < N_A < 0.083$. For values of N_A larger than 0.05 or 0.083, respectively, the layer is unconditionally stable. For values of N_A smaller than these values, the gas–liquid system may be marginally unstable for adsorption of surface-tension-increasing solute ($\beta < 0$, $\alpha < 0$) as well as in the case of desorption of surface-tension-decreasing solute ($\beta > 0$, $\alpha > 0$).

Figures 1 and 2, reproduced from Brian's work (21), give the critical Marangoni number versus N_A for different values of the Biot number in the conducting and insulating cases, respectively.

It is well known that the linear theory does not predict the shape of the convective cells. To determine the geometry of the pattern, one needs to proceed to the second-order solution of the problem.

3.2. *Second-Order Solution*

We select a planform function consisting of two horizontal space modes of the same overall wave number a with two amplitudes depending on time, namely

$$\Phi(x, y, t) = Z(t)\cos ay + Y(t)\cos any \cos amx. \quad [34]$$

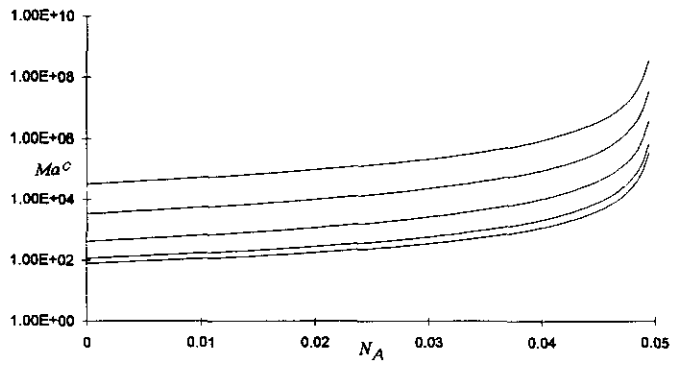

FIG. 1. Critical Marangoni number versus adsorption number in the conducting case. The values of the Biot number are 0, 1, 10, 100, 1000; the lower curve represents the lower Biot number.

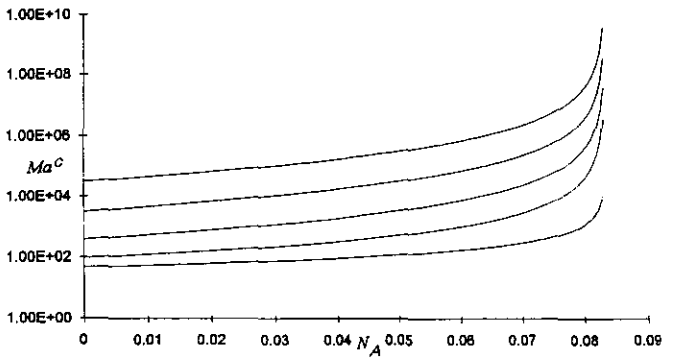

FIG. 2. Critical Marangoni number versus adsorption number in the insulating case. The values of the Biot number are 0, 1, 10, 100, 1000; the lower curve represents the lower Biot number.

$Z(t)$ and $Y(t)$ are two unknown time-dependent amplitudes and m and n are given, respectively, by

$$m = \sqrt{3}/2, \quad n = 1/2. \quad [35]$$

For $Y = 0$ and $Z =$ constant, the pattern consists of rolls while for $Y = \pm 2Z$, it consists of hexagonal cells.

The second-order solution is obtained by integrating the inhomogeneous set [22] $n = 2$. Existence of nontrivial solutions is ensured by the Fredholm condition, stating that

$$\langle \mathbf{u}^*, [\mathbf{N} + (\mathrm{Ma} - \mathrm{Ma}^c)\mathbf{M}](\mathbf{u}^{(1)}) \rangle = 0, \quad [36]$$

where

$$\mathbf{u}^* = [w^*(x, y, z, t), c^*(x, y, z, t), c^*(x, y, 1, t)] \quad [37]$$

is the solution of the linear adjoint problem, which is made explicit in Appendix A. The orthogonality condition [36] imposes that the amplitudes $Y(t)$ and $Z(t)$ satisfy

$$\dot{Y} = L\epsilon Y - \gamma YZ, \quad \dot{Z} = L\epsilon Z - \frac{\gamma}{4} Y^2,$$

where an overdot means derivation with respect to time and the coefficient L depend generally on Bi and N_A.

The second-order solution $\mathbf{u}^{(2)} = [w^{(2)}(x, y, z, t), c^{(2)}(x, y, z, t), c^{(2)}(x, y, 1, t)]$ obeys the equations and boundary conditions

$$\nabla^2 c^{(2)} + w^{(2)} = C_1\dot{\Phi} + DW_1C_1(\Phi_0 + \tfrac{1}{2}\Phi_2 - \tfrac{1}{2}\Phi_3 - \Phi_4) + DC_1W_1(\Phi_0 + \Phi_2 + \Phi_3 + \Phi_4), \quad [38]$$

with

$$\nabla^4 w^{(2)} = 0, \quad [39]$$

$$\text{at } z = 1: \quad \begin{matrix} \partial_{zz} w^{(2)} - \mathrm{Ma}^c \nabla_1^2 c^{(2)} = \epsilon \mathrm{Ma}^c \nabla_1^2 c^{(1)}, \\ w^{(2)} = 0, \ \partial_z c^{(2)} + \mathrm{Bi}\, c^{(2)} = N_A \partial_z w^{(2)}, \end{matrix} \quad [40]$$

$$\text{at } z = 0: \ w^{(2)} = \partial_z w^{(2)} = 0,$$

$$c^{(2)} = 0 \quad \text{or} \quad \partial_z c^{(2)} = 0. \quad [41]$$

$\dot{\Phi}$ is given by

$$\dot{\Phi} = \dot{Z}(t)\cos ay + \dot{Y}(t)\cos amx \cos any,$$

while the functions Φ_i ($i = 0, 2, 3, 4$) appearing in [38] are defined by

$$\Phi_0 = \frac{Z^2(t)}{2} + \frac{Y^2(t)}{4}, \quad [42]$$

$$\Phi_2 = \frac{Y^2(t)}{4}\cos ay + Y(t)Z(t)\cos amx \cos any, \quad [43]$$

$$\Phi_3 = \frac{Y^2(t)}{4}\cos 2amx + Y(t)Z(t)\cos amx \cos 3any, \quad [44]$$

$$\Phi_4 = \frac{Z^2(t)}{2}\cos 2ay + \frac{Y^2(t)}{4}\cos 2amx \cos ay. \quad [45]$$

The solution of the set [38]–[41] may be written in the form

$$w^{(2)} = W_3(z)\Phi_3 + W_4(z)\Phi_4, \quad [46]$$

$$c^{(2)} = H(z)\dot{\Phi} + C_0(z)\Phi_0 + C_2(z)\Phi_2 + C_3(z)\Phi_3 + C_4(z)\Phi_4, \quad [47]$$

where the unknown functions are made explicit in Appendix B.

The application of the Fredholm condition [36] on the set [38]–[41] results in

$$\iiint_V c^*[\partial_t c^{(1)} + (\mathbf{u}^{(1)} \cdot \nabla c^{(1)}) + (\mathbf{u}^{(1)} \cdot \nabla c^{(2)}) + (\mathbf{u}^{(2)} \cdot \nabla c^{(1)})]dV + \epsilon \mathrm{Ma}^c \iint_{S(z=1)} \partial_z w^* \nabla_1^2 c^{(1)} dS = 0. \quad [48]$$

In [48] only two integrals proportional to $\cos^2 ay$ and $\cos^2 amx \cos^2 any$ are not zero and they give rise to the third-order amplitude equations

$$\dot{Y} = L\epsilon Y - \gamma YZ - RY^3 - PYZ^2, \quad [49]$$

$$\dot{Z} = L\epsilon Z - \frac{\gamma}{4}Y^2 - R_1 Z^3 - \frac{P}{2}Y^2 Z, \quad [50]$$

where the values of the coefficients L, γ, R_1, P, and $R = (P + R_1)/4$ depend generally on the adsorption and Biot numbers. By deriving relations [49] and [50], it was assumed that the function $\dot{\Phi}$ was proportional to $\gamma\Phi_2$. This assumption, which allows terms containing $\dot{Y}$ and $\dot{Z}$ to be eliminated, does not influence the stability of the steady solutions of [49] and [50], when $L\epsilon$ and γ are small; this property was proved by Segel and Stuart (35). The remaining problem consists in finding the steady solutions of [49] and [50] and analyzing their stability with respect to small disturbances. Each steady solution represents either a state of diffusion without convection or a convective roll, hexagonal, or hybrid cell. Their stability will depend on the value of the parameter $\epsilon = \mathrm{Ma} - \mathrm{Ma}^c/\mathrm{Ma}^c$.

4. RESULTS AND DISCUSSION

In Fig. 3 the coefficient L versus the adsorption number for both the conducting and the insulating cases and two different values of the Biot number is plotted. The factor L expresses the linear growth of the disturbance. For the same value of Bi, we notice that the conducting case is the most unstable. The presence of an *adsorption barrier* beyond which the layer is unconditionally stable is also illustrated in Fig. 3. For the conducting case: it is seen that the N_A limit is 0.05 and for the insulating case it is 0.083. These results are in full agreement with Brian's linear theory (21).

Figure 4 represents the coefficient γ versus the adsorption number with the same values of the Biot number as in Fig. 3. It is noticed that the γ values for the conducting case are greater in absolute value than those for the insulating case.

The behavior of the coefficients P and R_1 for the conducting case, together with Bi = 0 and 1, is given in Fig. 5. In Fig. 6 the coefficients P and R_1 for the insulating case and Bi = 1, 2 are represented. Comparison of Figs. 5 and 6 shows that the coefficients of the amplitude equations are considerably smaller in the insulating case; moreover these values

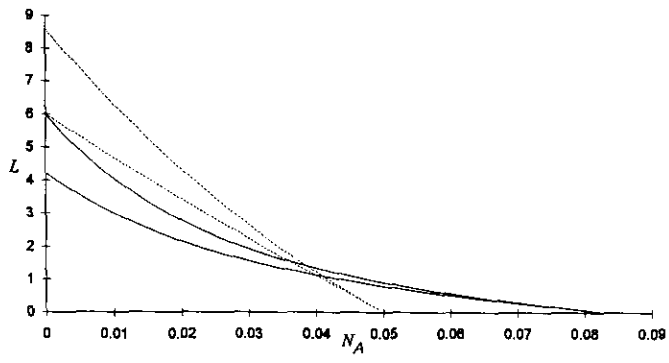

FIG. 3. Coefficient L versus adsorption number. In the conducting case (dashed line), the values of the Biot number are 0 and 1. In the insulating case (continued line), the values of the Biot are 1 and 2. In each case, the lower curve represents the lower Biot number.

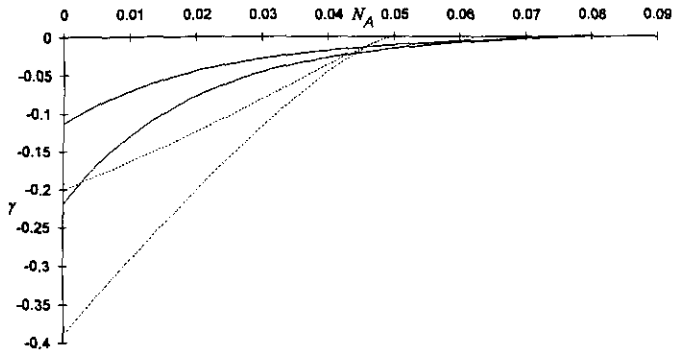

FIG. 4. Coefficient γ versus adsorption number. In the conducting case (dashed line), the values of the Biot are 0 and 1. In the insulating case (continued line), the values of the Biot are 1 and 2. In each case, the lower curve represents the higher Biot number.

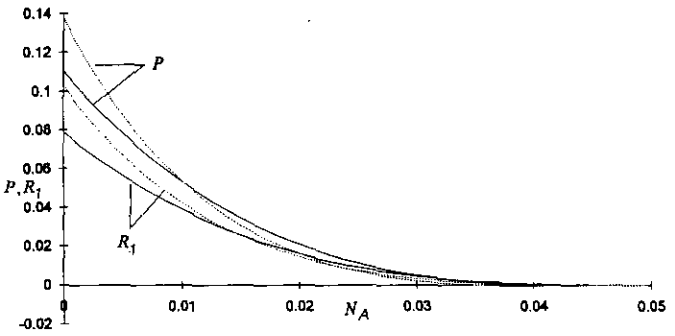

FIG. 5. Coefficients P and R_1 versus adsorption number in the conducting case. The Biot values are 0 (continued line) and 1 (dashed line).

grow with the Biot number. It should be noticed that for $Na = 0.05$ (0.0833) in the conducting (respectively insulating) case, the coefficients L, γ, P, R_1, and R tend to zero.

Knowledge of the values of L, γ, P, R_1, and R allows one to determine which of the equilibrium solutions (so-called fixed points) of the system in [49] and [50] are stable or unstable according to the value of ϵ. The analysis of both differential equations is well known from the work by Segel and Stuart (35) and we recall here just the essential points.

The main problem consists of finding the equilibrium solutions of the system in [49] and [50] and analyzing their stability with respect to small disturbances. There are nine fixed points, namely

$$\text{I: } Y = Z = 0 \qquad [51]$$

$$\text{IIa, b: } Y = 0,\ Z = \pm(\epsilon L/R_1)^{1/2}, \qquad [52]$$

$$\text{IIIa, b: } Y = 2Z,$$

$$Z = (2T)^{-1}[-\gamma \pm (\gamma^2 + 4\epsilon LT)^{1/2}], \qquad [53]$$

$$\text{IVa, b: } Y = -2Z,$$

$$Z = (2T)^{-1}[-\gamma \pm (\gamma^2 + 4\epsilon LT)^{1/2}], \qquad [54]$$

$$\text{Va, b: } Z = -\gamma/Q,\ Y = \pm R^{-1/2}[\epsilon L - R_1\gamma^2 Q^{-2}]^{1/2}, \qquad [55]$$

where

$$T = P + 4R = 8R - R_1,$$

$$Q = P - R_1 = 2(2R - R_1). \qquad [56]$$

In [52]-[55], a plus sign corresponds to case a and a minus sign to case b.

Each fixed point has a physical meaning. Solution I corresponds to a diffusive (motionless) state. Solutions II exist for nonzero R_1 and positive values of $\epsilon L/R_1$ and represent cells of two-dimensional planform (rolls). Fixed points III and IV are obtained for $\epsilon > \epsilon_c = \gamma^2/4LT$ when T is positive and for $\epsilon < \epsilon_c$ if T is negative. They form a hexagonal planform. It is not necessary to consider solutions III and IV separately, because the system in [49] and [50] is invariant under the transformation $Y' = -Y$. Solutions V are defined for $\epsilon \geqslant \epsilon_1 = \gamma^2 R_1/LQ^2$ and nonzero values of R and Q. They represent so-called hybrid cells if $\epsilon > \epsilon_1$ and rolls for $\epsilon = \epsilon_1$.

For thermocapillary convection in a liquid layer the coefficients L, P, R, R_1, and T are positive with in addition $T > Q$. A stability analysis of the corresponding solutions was carried out in (32). The results remain valid here under the above-mentioned restrictions on the coefficients; they are summarized in Table 1, where ϵ_2 is given by $\epsilon_2 = \gamma^2(T - Q)/LQ^2$. It was shown that hexagons are stable configurations for sufficiently small positive values of ϵ and for some negative values (subcritical instability); rolls are preferred modes for sufficiently large values of ϵ. It was also observed that the stable hexagonal cells are those with the fluid rising at the center (IIIa and IVa).

The difference between thermal and the solutal capillary convections is that in the latter case, the quantities P, R, and R_1, as well as Q and T, vary with the adsorption number

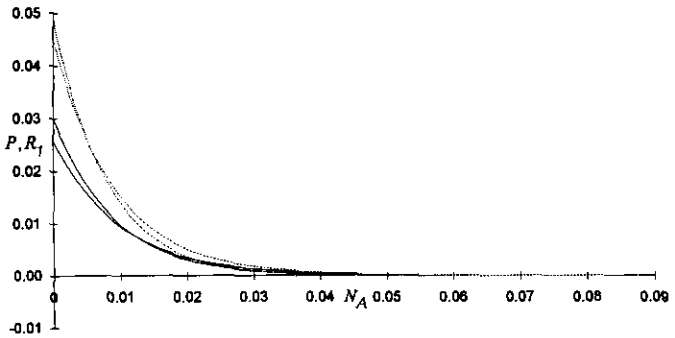

FIG. 6. Coefficients P and R_1 versus adsorption number in the insulating case. The Biot values are 1 (continued line) and 2 (dashed line). The coefficient P is greater than R_1 at the origin.

TABLE 1
Stable Configurations According to the ϵ Values for $Q > 0$ and $T > 0$

$\epsilon = \frac{Ma - Ma^c}{Ma^c}$	Stable configurations ($N_A < N_A^Q$)
$\epsilon < \epsilon_c$	Conductive state
$\epsilon_c < \epsilon < 0$	Conductive state, hexagons (subcritical range)
$0 < \epsilon < \epsilon_1$	Hexagons
$\epsilon_1 < \epsilon < \epsilon_2$	Hexagons, rolls
$\epsilon > \epsilon_2$	Rolls, hybrid cells

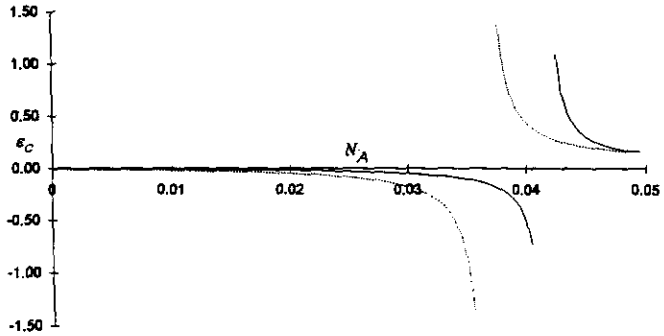

FIG. 8. Coefficient ϵ_c versus adsorption number in the conducting case. The Biot number are 0 (continued line) and Bi = 1 (dashed line).

and may take positive or negative values. Therefore a more detailed analysis is required.

As a preliminary we study the behavior of the coefficients ϵ_c, ϵ_1, and ϵ_2 as a function of N_A, for fixed Bi values.

In the insulating case, the quantity T is positive for all values of N_A and hence the coefficient ϵ_c is negative as seen in Fig. 7 displaying ϵ_c for different values of Bi. The absolute value of this coefficient increases with the adsorption number, reaches a maximum value, and afterward decreases. This results in an enlargement of the subcritical domain where convective patterns are observed for values of the Marangoni number smaller than the critical number Ma_c predicted by the linear stability theory.

In the conducting case, the sign of T changes at some value of N_A (say N_A^T) while ϵ_c, which is negative for $N_A < N_A^T$, becomes positive above that value. The corresponding ϵ_c vs N_A curves shown in Fig. 8 have a vertical asymptote at $N_A^T = 0.041$ for Bi = 0 and $N_A^T = 0.036$ for Bi = 1.

It should be mentioned that $\epsilon_c = -1$ corresponds to a zero Marangoni number and this means that instabilities could occur without any concentration gradient. In view of this physically irrelevant result, one must consider with caution the results corresponding to $\epsilon_c \leqslant -1$ as well as these obtained for large positive values of ϵ_c, because our analysis, which is restricted to third-order terms in the amplitude equations, is clearly satisfactory only for small ϵ values.

It is seen from Figs. 9 and 10 that in both insulating and conducting cases, the quantity Q is zero at some value of N_A (denoted N_A^Q); similarly a net increase of ϵ_1 and ϵ_2 is observed in the vicinity of that value. The coefficients ϵ_1 and ϵ_2 are plotted versus the adsorption number in Fig. 11 for the insulating case and in Fig. 12 for the conducting case. In the former case both quantities are positive, and in the latter case their sign changes from positive to negative and ϵ_1 vanishes at some value (say N_A^{R1}), where $R_1 = 0$; concerning ϵ_2, it is found that ϵ_2 is zero when $T = Q$. The present stability analysis is certainly not valid in the vicinity of N_A^Q, but is valid for values of N_A sufficiently far from N_A^Q, where the N_A values remain small.

We are now in position to examine the stability of the fixed points [51]–[55].

(i) Let us start with the *insulating* case. For $N_A < N_A^Q$, the stable configurations are these reported in Table 1. For $\epsilon > \epsilon_1$, it is observed that rolls and hexagons given by solution IIIa (and IVa) are stable simultaneously. There exists also a small subcritical domain in which hexagons coexist with the static state as in the problem of thermocapillary convection.

For $Q < 0$, i.e., in the interval $(N_A^Q, 0.083)$, the stable configurations are presented in Table 2. Rolls are no longer

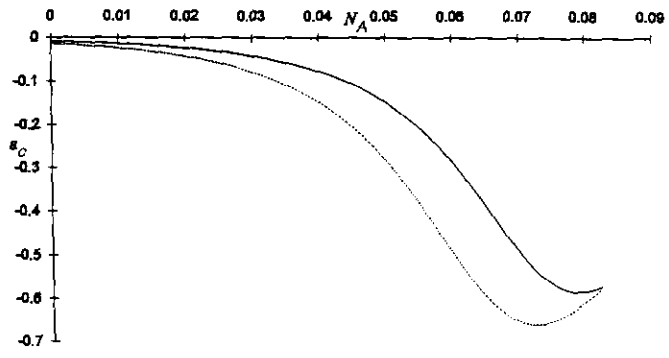

FIG. 7. Coefficient ϵ_c versus adsorption number, in the insulating case. The Biot values are 1 (continued line) and Bi = 2 (dashed line).

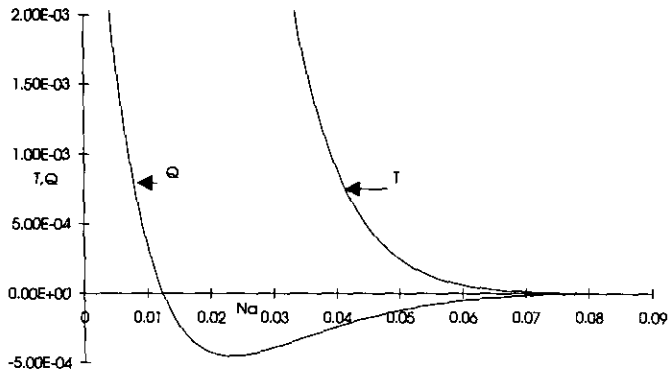

FIG. 9. Coefficients T and Q versus adsorption number at Bi = 1 (insulating case).

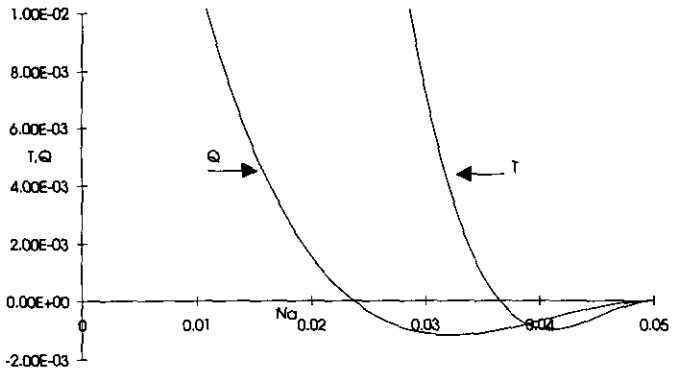

FIG. 10. Coefficients T and Q versus adsorption number at Bi = 1 (conducting case).

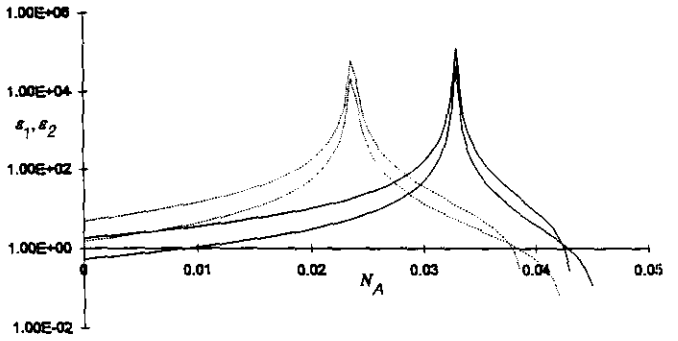

FIG. 12. Coefficients ϵ_1, ϵ_2 versus adsorption number in the conducting case. The Biot values are 0 (continued line) and Bi = 1 (dashed line).

stable but hybrid cells are possible patterns for $\epsilon_1 < \epsilon < \epsilon_2$. Hexagons IIIa and IVa are stable for $\epsilon > \epsilon_c$, while solutions IIIb and IVb are stable for $\epsilon > \epsilon_2$. The subcritical domain enlarges with increasing adsorption number, thus displaying critical Marangoni numbers which are $(1 + \epsilon_c)$ times smaller than those predicted by the linear stability theory. The minimum negative value of ϵ_c is equal to -0.57 at $N_A = 0.075$ for Bi = 1 and -0.66 at $N_A = 0.073$ for Bi = 2 (see Fig. 7).

(ii) In the *conducting* case, stable patterns are those displayed in Tables 1 and 2 for both signs of Q, provided $T > 0$, i.e., in the interval $(0, N_A^T)$. Considering negative values of Q, one has the sequence of inequalities $N_A^Q < N_A^T < N_A^R < N_A^{R1}$ which are obtained for the range of Biot's number used in this work. For example, for Bi = 0, one has $N_A^Q = 0.032$, $N_A^T = 0.041$, $N_A^R = 0.042$, $N_A^{R1} = 0.045$, and for Bi = 1, $N_A^Q = 0.023$, $N_A^T = 0.036$, $N_A^R = 0.037$, and $N_A^{R1} = 0.042$.

The results of the stability analysis for negative values of T are presented in Table 3. For $N_A^T < N_A < N_A^R$ stable configurations are hybrid cells in the interval (ϵ_1, ϵ_2) and hexagons IIIb and IVb in the interval (ϵ_2, ϵ_c).

In short, for $N_A^T < N_A < N_A^R$ hexagons and hybrid cells are the preferred modes in the interval (ϵ_1, ϵ_c) and the layer is unstable for other positive values of ϵ outside this range. Analysis shows that in the next interval $(N_A^R, 0.05)$ the system is unconditionally unstable whatever the positive value of ϵ. This result is not surprising because for $N_A > N_A^{R1}$, all the coefficients of the third-order terms of Eqs. [49] and [50] are negative.

One can summarize by saying that in the conducting case, and for positive values of ϵ, the layer is unstable with respect to two-amplitude disturbances when the adsorption number is larger than N_A^{R1}. This is in contrast with the linear theory, where it is found that the layer is unconditionally stable for $N_A > 0.05$. In the present work, the stability property is deeply influenced by the values of the parameters T and Q. These quantities are a combination of the third-order terms of the amplitude equations [49] and [50]. For small value of the adsorption number, both T and Q are positive and the system follows the hierarchy of states found in the Table 1. The increase of the adsorption number leads to a negative Q. The rolls become subcritical, which means that now the third-order terms are destabilizing. A new increase of the adsorption number leads to $T < 0$, at which both rolls and hexagons become subcritical; thus the third-order terms in the amplitude equations are now destabilizing both rolls and hexagons.

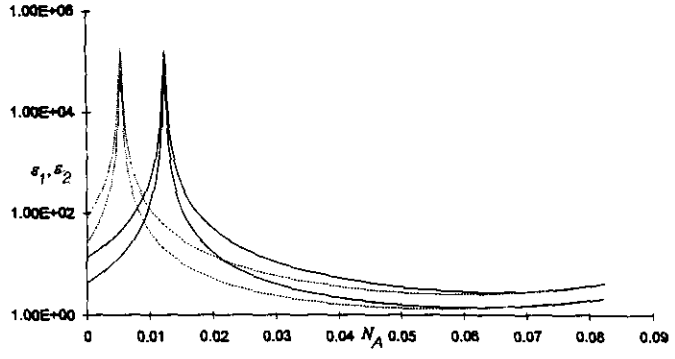

FIG. 11. Coefficients ϵ_1, ϵ_2 versus adsorption number in the insulating case. The Biot values are 1 (continued line) and Bi = 2 (dashed line).

5. SUMMARY AND FINAL COMMENTS

Nonlinear solutal Marangoni convection in a thin liquid layer is studied; the layer is bounded from below by a rigid

TABLE 2
Stable Configurations According to the ϵ Values for $Q < 0$ and $T > 0$

$\epsilon = \frac{Ma - Ma^c}{Ma^c}$	Stable configurations $(N_A^Q < N_A < 0.083)$
$\epsilon < \epsilon_c$	Conductive state
$\epsilon_c < \epsilon < 0$	Conductive state, hexagons
$0 < \epsilon < \epsilon_1$	Hexagons
$\epsilon_1 < \epsilon < \epsilon_2$	Hexagons, hybrid cells
$\epsilon > \epsilon_2$	Hexagons

TABLE 3
Stable Configurations According to the ϵ Values for $Q < 0$, $T < 0$, and $R > 0$

$\epsilon = \frac{Ma - Ma^c}{Ma^c}$	Stable configurations $(N_A^T < N_A < N_A^R)$
$\epsilon < 0$	Conductive state
$0 < \epsilon < \epsilon_1$	No stable configuration
$\epsilon_1 < \epsilon < \epsilon_2$	Hybrid cells
$\epsilon_2 < \epsilon < \epsilon_c$	Hexagons
$\epsilon > \epsilon_c$	No stable configuration

wall and from above by a free surface subject to adsorption/desorption of a surface-active solute. The Gibbs adsorption mechanism is assumed.

A finite amplitude method is used and leads to a set of two nonlinear differential equations with coefficients depending strongly on the adsorption number N_A. The value of N_A will determine the nature of the convective patterns in the layer.

The present work is an extension of an earlier contribution by Brian (21), who considered infinitesimally small amplitude disturbances. According to Brian's linear theory, there exists a critical value of the adsorption number above which the system is unconditionally stable. The present nonlinear analysis indicates that the results of the linear theory seem too crude. Indeed it is found that above some value of the adsorption number, the two-amplitude nonlinear terms have a destabilizing effect. The predicted values of the critical Marangoni number are reduced in comparison with the result obtained from the linear theory. A domain of subcritical instability is also displayed.

The present analysis presents strong analogies with the corresponding thermal Marangoni problem, where instability is driven by a temperature-dependent surface tension. In both solutal and temperature Marangoni convections, hexagonal cells are predicted as soon as Ma is larger than its critical value Ma^c. By increasing Ma, roll patterns are expected depending on the values of the parameters. A domain of subcritical instability at $Ma < Ma^c$ is also displayed. These theoretical results predicting that hexagonals cells will emerge are to a given extent verified by some experiments (24, 25) where polygonal cells, but not perfect hexagons, are observed at the onset of convection.

It must be kept in mind that the present model is a simplified one and provides only a first step toward a more complete analysis. Several important phenomena like deformability of the upper surface and the effect of lateral walls have not been taken into account. It is well known that by assuming the upper surface planar and undeformable, interesting film thinning and rupture phenomena are left out. Another problem is related to the omission of the nonlinear surface convection terms in the mass balance [16]; to check quantitatively the validity of such an assumption, it would be interesting to repeat the preceding analysis by including these nonlinearities.

APPENDIX A

Solution of the Linear Adjoint Problem

The linear problem may be written in the form

$$[\mathbf{L} - Ma^c\mathbf{M}](\mathbf{u}) = 0. \qquad [A1]$$

The boundary condition involving the Marangoni number Ma has been included in vector formulation [A1]; the remaining boundary conditions are

$$w = \partial_z c + Bi\, c - N_A \partial_z w = 0, \quad \text{at } z = 1 \qquad [A2]$$

$$w = \partial_z w = \partial_z c + hc = 0, \quad \text{at } z = 0. \qquad [A3]$$

The adjoint operator is defined by

$$\langle \mathbf{u}^*, [\mathbf{L} - Ma^c\mathbf{M}](\mathbf{u})\rangle = \langle \mathbf{u}, [\mathbf{L}^* - Ma^c\mathbf{M}^*](\mathbf{u}^*)\rangle, \qquad [A4]$$

where $\mathbf{u}^* = (w^*, c^*, \partial_z w^* (z = 1))$ is the adjoint eigenvalue vector solution of

$$[\mathbf{L}^* - Ma^c\mathbf{M}^*](\mathbf{u}^*) = 0. \qquad [A5]$$

By integration by parts of the left-hand side of [A4] and use of [A2] and [A3], one obtains

$$[\mathbf{L}^* - Ma^c\mathbf{M}^*] = \begin{bmatrix} \nabla^4 & 1 & 0 \\ 0 & \nabla^2 & 0 \\ 0 & (\partial_z + Bi)|_{z=1} & Ma^c\nabla_1^2 \end{bmatrix}, \qquad [A6]$$

with the corresponding adjoint boundary conditions

$$w^* = \partial_z w^* = \partial_z c^* + hc^* = 0, \quad \text{at } z = 0,$$

$$w^* = \partial_{zz} w^* + N_A c^* = 0, \quad \text{at } z = 1. \qquad [A7]$$

By analogy with the linear problem, let us separate the variables and write the solutions of the problem in the form

$$w^* = W^*(z)\Phi(x, y, t),$$

$$c^* = C^*(z)\Phi(x, y, t). \qquad [A8]$$

To compute the Fredholm condition it is necessary to calculate $C^*(z)$ and $DW^*(1)$. For the conducting case ($C^*(0) = 0$) the solution is given by

$$C^*(z) = A^*\sinh az,$$

$$DW^*(1) = A^*(a\cosh a + \mathrm{Bi}\sinh a)/a^2\mathrm{Ma}. \quad [A9]$$

For the insulating case ($\partial_z c^*(0) = 0$), one has

$$C^*(z) = A^*\cosh az,$$

$$DW^*(1) = A^*(a\sinh a + \mathrm{Bi}\cosh a)/a^2\mathrm{Ma}. \quad [A10]$$

In [A9] and [A10] the factor A^* is an arbitrary constant, which is of no importance in the present analysis.

APPENDIX B

Second-Order Solution

The problem amounts to solving linear equations [38] and [39] associated with boundary conditions [40] and [41]. The solution is given by expressions [46] and [47], in which the unknown functions $W_3(z)$, $W_4(z)$, $H(z)$, $C_1(z)$, $C_2(z)$, $C_3(z)$, and $C_4(z)$ satisfy relevant equations and boundary conditions. It was proved that the terms in $w^{(2)}$ which are related to $\dot{\Phi}$, Φ_1, and Φ_2 are zero. The functions $W_3(z)$ and $W_4(z)$ are solutions of Eq. [25] with boundary conditions [27] and [28] at the condition to replace in W_3 wave number a by $a\sqrt{3}$ and in W_4 quantity a by $2a$. W_3 and W_4 have the same form as in [29] with unknown constants A_3 and A_4 (instead of A) to be determined later together with the functions $C_3(z)$ and $C_4(z)$.

The function $C_0(z)$ satisfies the equation and boundary conditions

$$D^2C_0 = (DW)_1C_1 + (DC_1)W_1 \equiv F_0(z), \quad [B1]$$

$$DC_0 = 0 \quad \text{at } z = 0 \text{ (insulating surface)} \quad [B2]$$

$$DC_0 + \mathrm{Bi}C_0 = 0 \quad \text{at } z = 1. \quad [B3]$$

After applying the Green function method, the above system may be written in the form

$$C_0(z) = \int_0^z \left(z - \frac{\mathrm{Bi}+1}{\mathrm{Bi}}\right)F_0(u)du + \int_z^1 \left(u - \frac{\mathrm{Bi}+1}{\mathrm{Bi}}\right)F_0(u)du. \quad [B4]$$

Since the functions $\dot{\Phi}$ and Φ_2 contain two terms, one proportional to cos ay and the other to cos amx cos any, the corresponding functions $H(z)$ and $C_2(z)$ consist also of two terms. The sum of the terms of $H(z)$ and $C_2(z)$ (say $\tilde{C}(z)$) which are related to cos ay satisfies the relation

$$(D^2 - a^2)\tilde{C} = C_1\dot{Z} + \frac{Y^2}{4} \times \left(W_1DC_1 + \frac{1}{2}DW_1C_1\right) \equiv \tilde{F}(z, t) \quad [B5]$$

and boundary conditions [B2] and [B3]. The solution for the conducting case ($C_0 = 0$ at $z = 0$) is obtained by following the same Green function procedure; it is found that

$$\tilde{C}(z) = \int_0^z G_1(z, u)\tilde{F}(u)du + \int_z^1 G_2(z, u)\tilde{F}(u)du, \quad [B6]$$

$$G_1(z, u) = \frac{\sinh au}{a\cosh a + \mathrm{Bi}\sinh a} \times \left\{\frac{\mathrm{Bi}}{a}\sinh[a(z-1)] - \cosh[a(1-z)]\right\},$$

$$G_2(z, u) = \frac{\sinh az}{a\cosh a + \mathrm{Bi}\sinh a} \times \left\{\frac{\mathrm{Bi}}{a}\sinh[a(u-1)] - \cosh[a(1-u)]\right\}. \quad [B7]$$

The sum of the terms in $H(z)$ and $C_2(z)$ which correspond to cos amx cos any is denoted $\tilde{\tilde{C}}(z)$ and obeys the equation

$$(D^2 - a^2)\tilde{\tilde{C}} = \dot{Y}C_1 + YZ(W_1DC_1 + \tfrac{1}{2}DW_1C_1) \equiv \tilde{\tilde{F}}, \quad [B8]$$

together with boundary conditions [B2] and [B3]. The solution is given by expression [B6], in which $\tilde{F}$ is replaced by $\tilde{\tilde{F}}$. The functions $\tilde{F}$ and $\tilde{\tilde{F}}$ are tilted because the time appears as a parameter in [B5]–[B8].

The function $C_3(z)$ is the solution of the problem ($k = a\sqrt{3}$)

$$(D^2 - k^2)C_3 = -W_3 + DC_1W_1 - \tfrac{1}{2}DW_1C_1 \equiv F_3(z), \quad [B9]$$

$$D^2W_3 + k^2\mathrm{Ma}^cC_3 = 0, \quad \text{at } z = 1, \quad [B10]$$

$$DC_3 + \mathrm{Bi}C_3 = N_ADW_3, \quad \text{at } z = 1, \quad [B11]$$

$$C_3 = 0, \quad \text{at } z = 0, \quad [B12]$$

and is given by

$$C_3(z) = \int_0^z G_1(z, u)F_3(u)du + \int_z^1 G_2(z, u)F_3(u)du + \frac{N_ADW_3(1)\sinh kz}{[k\cosh k + \mathrm{Bi}\sinh k]}. \quad [B13]$$

The functions G_1 and G_2 are still given by [B7], where a is replaced by k. The constant A_3 is found from boundary condition [B10].

The function $C_4(z)$ satisfies problem [B9]–[B12] with $k = 2a$ and $F_4(z) = -W_4 + DC_1W_1 - DW_1C_1$ instead of $F_3(z)$ and has the same form as $C_3(z)$.

ACKNOWLEDGMENTS

This text presents partial research results of the Belgian program on Interuniversity Pole of Attraction (PAI n°21) initiated by the Belgian State, Prime Minister's Office, Science Policy Programming. Support of the European Community (Human Capital and Mobility) under Grant ERB CHRXCT 940 481 is also acknowledged.

REFERENCES

1. Ward, F. H., and Brooks, L. H., *Trans. Faraday Soc.* **48,** 1124 (1952).
2. Sawistowski, H., *in* "Recent Advances in Liquid–Liquid Extraction" (C. Hanson, Ed.). Pergamon Press, Oxford, 1971.
3. Linde, H., Schwartz, P., and Wilke, H., *in* "Dynamic and Instability of Fluid Interfaces" (T. S. Sorensen, Ed.), Lecture Notes in Physics, No. 105, p. 75. Springer-Verlag, Berlin, 1979.
4. Sternling, C. V., and Scriven, L. E., *AIChE J.* **5,** 514 (1959).
5. Cross, M. C., and Hohenberg, P. C., *Rev. Mod. Phys.* **65,** 851 (1993).
6. Linde, H., *in* "Convective Transport and Instability Phenomena" (J. Zierep and H. Oertel, Jr., Eds.), p. 265. Braun, Karlsruhe, 1982.
7. Orell, A., and Westwater, J. W., *Chem. Eng. Sci.* **16,** 127 (1961).
8. Brian, P. L. T., Vivian, J. F., and Matiatos, D. C., *AIChE J.* **13,** 28 (1967).
9. Hennenberg, M., Sorensen, T. S., and Sanfeld, A., *J. Chem. Soc. Faraday 2* **73,** 48 (1977).
10. Sorensen, T. S., Nielsen, J., Hennenberg, M., and Hansen, F. Y., *J. Chem. Soc. Faraday 2* **73,** 1589 (1977).
11. Sorensen, T. S., Hennenberg, M., and Hansen, F. Y., *J. Chem. Soc. Faraday 2* **74,** 1005 (1978).
12. Sorensen, T. S., *in* "Dynamic and Instability of Fluid Interfaces" (T. S. Sorensen, Ed.), Lecture Notes in Physics, No. 105. Springer-Verlag, Berlin, 1979.
13. Sorensen, T. S., *in* "Convective Transport and Instability Phenomena" (J. Zierep and H. Oertel, Jr., Eds.), p. 339. Braun, Karlsruhe, 1982.
14. Hennenberg, M., Sorensen, T. S., Steinchen, A., and Sanfeld, A., *J. Chim. Phys.* **72,** 1202 (1975).
15. Sorensen, T. S., Hennenberg, M., Steinchen, A., and Sanfeld, A., *J. Colloid Interface Sci.* **56,** 191 (1976).
16. Sorensen, T. S., *J. Chem. Soc. Faraday Trans.* **76,** 1170 (1980).
17. Sorensen, T. S., and Castillo, J., *J. Colloid Interface Sci.* **76,** 399 (1980).
18. Dalle Vedove, W., and Sanfeld, A., *J. Colloid Interface Sci.* **84,** 318, 328 (1981).
19. Ibanez, J. L., and Velarde, M. G., *J. Phys.* **38,** 1479 (1977).
20. Pearson, J. R. A., *J. Fluid Mech.* **4,** 489 (1958).
21. Brian, P. L. T., *AIChE J.* **17,** 765 (1971).
22. Brian, P. L. T., and Smith, K. A., *AIChE J.* **18,** 231 (1972).
23. Brian, P. L. T., and Ross, J. R., *AIChE J.* **18,** 582 (1972).
24. Imaishi, N., Suzuki, Y., Hozawa, M., and Fujinawa, K., *Int. Chem. Eng.* **22,** 659 (1982).
25. Imaishi, N., Suzuki, Y., Hozawa, M., and Fujinawa, K., *Int. Chem. Eng.* **23,** 466 (1983).
26. Palmer, H., and Berg, J., *AIChEJ.* **19,** 1082 (1973).
27. Scanlon, J., and Segel, L., *J. Fluid Mech.* **30,** 149 (1967).
28. Kraska, J., and Sani, R., *Int. J. Heat Mass Transfer* **22,** 535 (1979).
29. Rosenblat, S., Davis, S. H., and Homsy, G., *J. Fluid Mech.* **120,** 91 (1982).
30. Cloot, A., and Lebon, G., *J. Fluid Mech.* **145,** 447 (1984).
31. Bragard, J., and Lebon, G., *Europhys. Lett.* **21,** 831 (1993).
32. Adamson, A. W., "Physical Chemistry of Surfaces." Interscience, New York, 1960.
33. Kozhoukharova, Zh. D., and Slavtchev, S. G., *J. Colloid Interface Sci.* **148,** 42 (1992).
34. Hennenberg, M., Bish, P., Vignes-Adler, M., and Sanfeld, A., *J. Colloid Interface Sci.* **69,** 128 (1979).
35. Segel, L. A., and Stuart, J. T., *J. Fluid Mech.* **13,** 289 (1962).